

Supplementary Information

Nitrogen-doped Graphene Interpenetrated 3-D Ni- Nanocage: Efficient and Stable

Water-to-Dioxygen Electrocatalyst

Vishal M. Dhavale,^{a,c} Sachin S. Gaikwad,^a Leena George,^{b,c} R. Nandini Devi,^{b,c} Sreekumar
Kurungot^{*ac}

^aPhysical and Materials Chemistry Division, CSIR-National Chemical Laboratory, Pune-411 008, India.

^bCatalysis and Inorganic Chemistry Division, CSIR-National Chemical Laboratory, Pune-411 008, India.

^cAcademy of Scientific and Innovative Research (AcSIR), Anusandhan Bhawan, 2 Rafi Marg, New Delhi-110001, India.

Fax: +91-20-25902636/2615; Tel: +91-20-25902566; E-mail: k.sreekumar@ncl.res.in

Content

| | |
|--|------------|
| 1. Experimental and Characterization Section | S3 |
| a) Synthesis of reduced graphene oxide (RGO)..... | S3 |
| b) Synthesis of N-doped graphene (NGr) | S3 |
| c) Synthesis of nickel-particles | S4 |
| d) Rotating ring disk electrode study | S4 |
| 2. Results | S5 |
| Figure S1: TEM image of RGO (Gr) and N-Gr | S5 |
| Figure S2a: HR-TEM image of Ni-NGr nanocage structures..... | S6 |
| Figure S2b: Line profile of the different edges of the Ni-NGr nanocage structure..... | S7 |
| Figure S3: Dark field image of Ni-NGr nanocage structure | S8 |
| Figure S4: SEM Elemental mapping of Ni-NGr nanocages structure | S9 |
| Figure S5: TEM image of Ni-Gr..... | S10 |
| Figure S6: Comparative Raman spectra of NiCl ₂ , RGO (Gr), NGr, Ni-NGr, physical mixture of NiCl ₂ +NGr..... | S11 |
| Figure S7: XPS of Ni of NiCl ₂ | S12 |
| Figure S8: XPS of C1s and O1s of Ni-NGr sample | S12 |
| Figure S9: XPS of N1s of the Ni-NGr sample | S13 |
| Figure S10: Deconvoluted XPS of C1s spectra of the NGr sample..... | S13 |
| Figure S11: Deconvoluted XPS of N1s spectra of the NGr sample | S14 |
| Figure S12: XPS of O1s spectra of the NGr sample | S15 |
| Figure S13: Cyclic voltammetry study, Tafel plot, and RRDE study of Ni-NGr..... | S16 |
| Figure S14: OER stability of NGr by LSV..... | S17 |
| Figure S15: Comparative LSV of Ni-Gr, Ni-particles, and Ni-NGr..... | S18 |
| Figure S16: Capacitive CV and graph of anodic and cathodic current vs. scan rate of Ni-Gr..... | S19 |
| 3. Mechanism of OER in alkaline medium | S20 |
| Table S1: Desorption energy per carbon atom (E_{des}) and activation energy (ΔE) for carbon diffusion of nickel surface | S20 |
| Table S2: Reported specific capacitance for Ni-based materials and platinum in alkaline medium | S21 |
| Table S3: Comparison of overpotential values for Ni-based electrocatalyst | S21 |
| 4. References | S22 |

1. Experimental and Characterization Section

a. Synthesis of reduced graphene oxide (RGO):

Synthesis of graphene oxide (GO): GO was synthesized by improved Hummer's method.¹ In short, a mixture of 3 g of graphite and required amount of KMnO_4 was added slowly into a 1 : 9 mixture of conc. H_3PO_4 : H_2SO_4 and the solution was kept under stirring for overnight by maintaining the reaction mixture temperature at 60 °C. The obtained solution was poured into ice cooled water containing 3% H_2O_2 . A yellow precipitate formed was separated by centrifugation at 10,000 rpm, and this was washed well with copious DI water. Finally, the product was washed with 30% HCl to remove unwanted impurities, followed by washing with ethanol and acetone. The product was allowed to dry at room temperature and this was used as such for the further studies.

Synthesis of RGO (Gr): GO was reduced by aqueous solution of sodium borohydride. Briefly, 50 mg of GO was dispersed in 50 ml DI water and this was transferred in a 250 ml round bottom flask and was kept under vigorous magnetic stirring for 30 min. 0.1 M sodium borohydride (25 ml) aqueous solution was added slowly through burette into the above mixture under stirring for 4 h. Finally, the reaction mixture was centrifuged at 10,000 rpm, washed with DI water and dried at 80 °C in an oven for 10 h. After that the product was annealed at 900 °C to remove maximum functional groups. The obtained black product is termed as RGO (Gr).

b. Synthesis of N-doped graphene (NGr):

1 g of RGO (Gr) was mixed with 6 g of melamine in 100 ml of DI water and the mixture was stirred for 24 h. The slurry was filtered and dried in an oven at 80 °C for overnight. The obtained melamine-Gr solid powder was heated at about 900 °C in an Argon atmosphere (flow rate: 0.2

slpm) for about 4 h. The furnace was cooled down to room temperature under inert atmosphere and the obtained N-Gr was used for the further investigations and synthesis of Ni-NGr structures.

c. Synthesis of nickel-particles:

Synthesis of Ni-particles: The Ni-particles are synthesized by chemical reduction method, for the comparison purpose. 25 mL (100 mM) nickel chloride solution was taken in 100 mL round bottom flask. Subsequently, 0.5 M aqueous solution of sodium borohydride was added slowly in the above nickel chloride solution. After complete addition, reaction mixture was kept under stirring for 8 h, and then, filtered with 0.2 μm polytetrafluoroethylene (PTFE) membrane filter paper. Finally, washed with DI water and dried in oven at 80 $^{\circ}\text{C}$ for 10 h.

d. Rotating ring disk electrode study:

For the rotating ring disk electrode (RRDE) measurements, the collection efficiency (N) of the electrode was determined by a standard ferrocene couple and the ratio of the ring and the disk limiting current gives the value of N. During the RRDE investigation, the ring potential was set to 1.3 V (vs. RHE).

To measure the faradaic efficiency (ϵ) of Ni-NGr for oxygen evolution reaction, measurement was done by applying a current step from 1 to 15 mA/cm^2 to the carbon disk and the corresponding voltage was measured. During the measurement, the rotation speed of the RRDE was kept at 1600 rotation per minutes (rpm). The faradaic efficiency was calculated by using Equation 1.¹⁷

$$\text{Faradaic efficiency } (\epsilon) = 2 \cdot I_r / I_d \cdot N \dots\dots\dots (\text{Equation 1})$$

where, I_r is the ring current, I_d is 2.7 mA, is the constant disk current for a 0.2646 cm² disk electrode to get minimum current density of 10 mA/cm² and N is the collection efficiency (0.37).

2. Results:

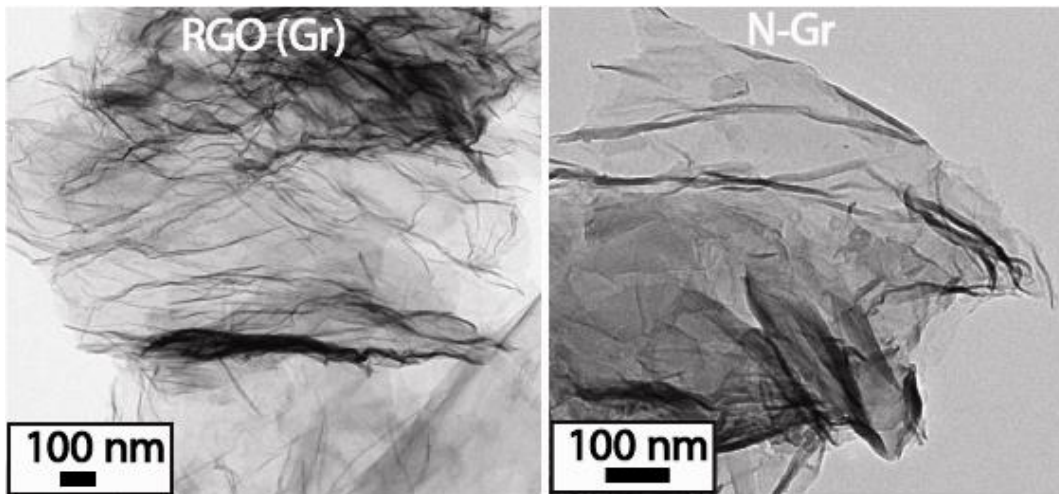


Figure S1: TEM images of (left) chemically reduced graphene oxide (Gr), and (right) N-doped graphene (NGr).

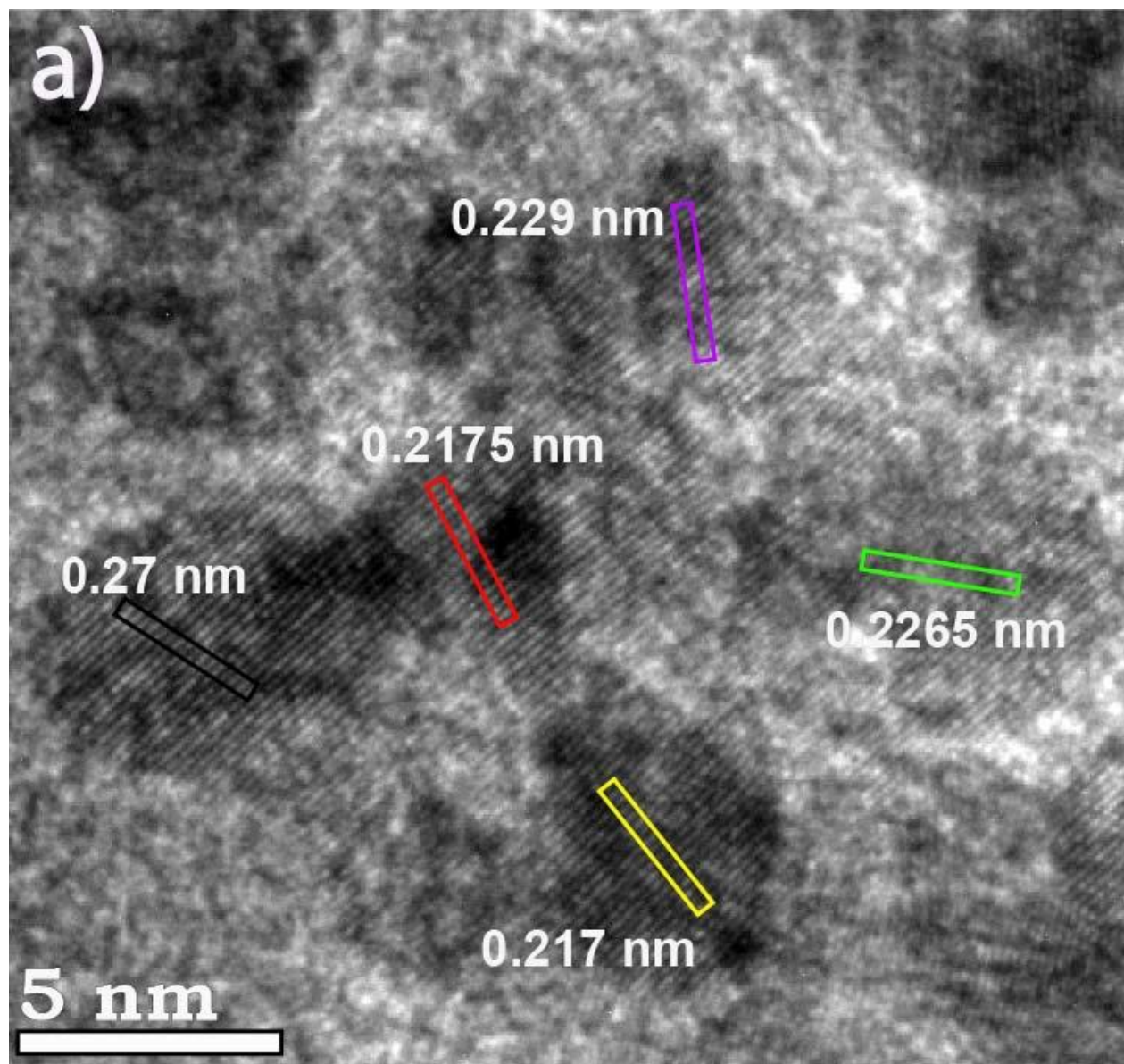


Figure S2a: HR-TEM image of Ni-NGr nanocage structure. Lattice fringes calculated at different edges and the corresponding line profiles are shown in Figure S2b with respective marked color.

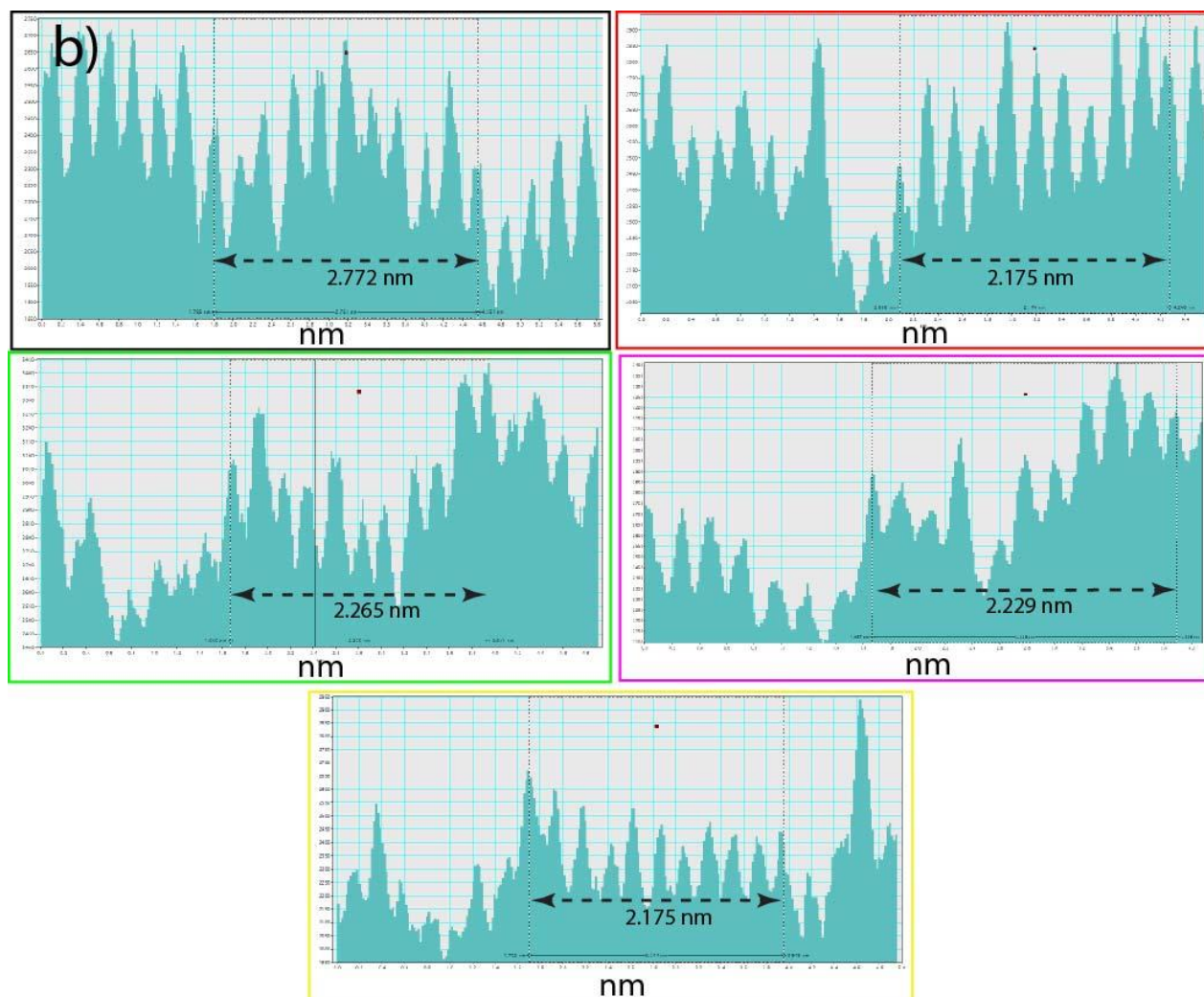


Figure S2b: Line profiles of the different edges of the Ni-NGr nanocage structure shown in Figure S2a. Lattice spacing values are ranging from 0.23-0.28 nm.

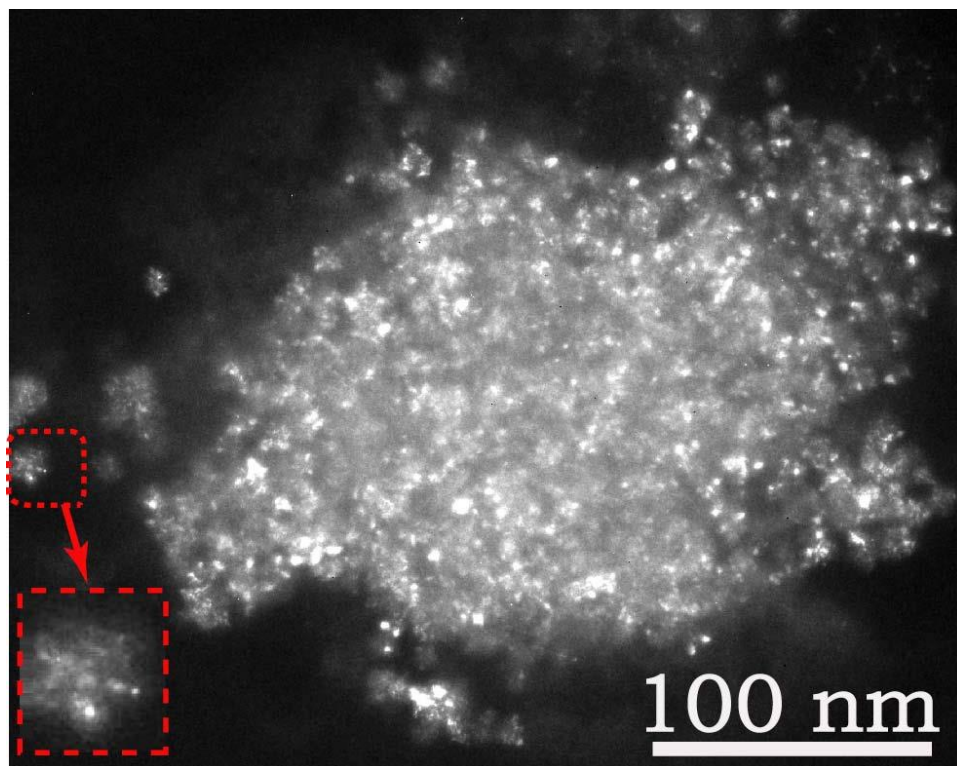


Figure S3: Dark field image of Ni-NGr. Inset shows the magnified image of a single Ni-NGr nanocage structure.

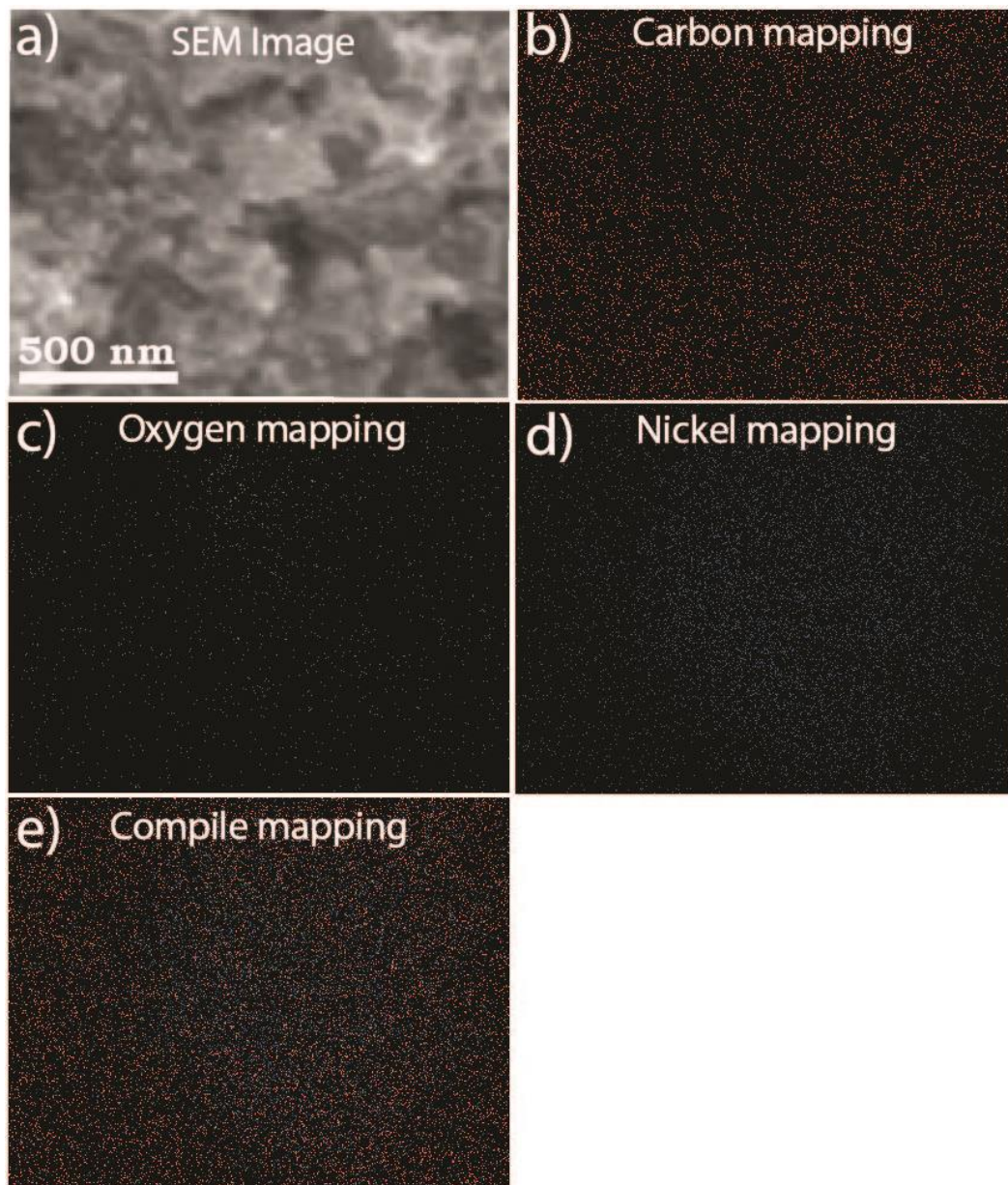


Figure S4: a) SEM image of Ni-NGr; b-e) SEM elemental mapping of the Ni-NGr.

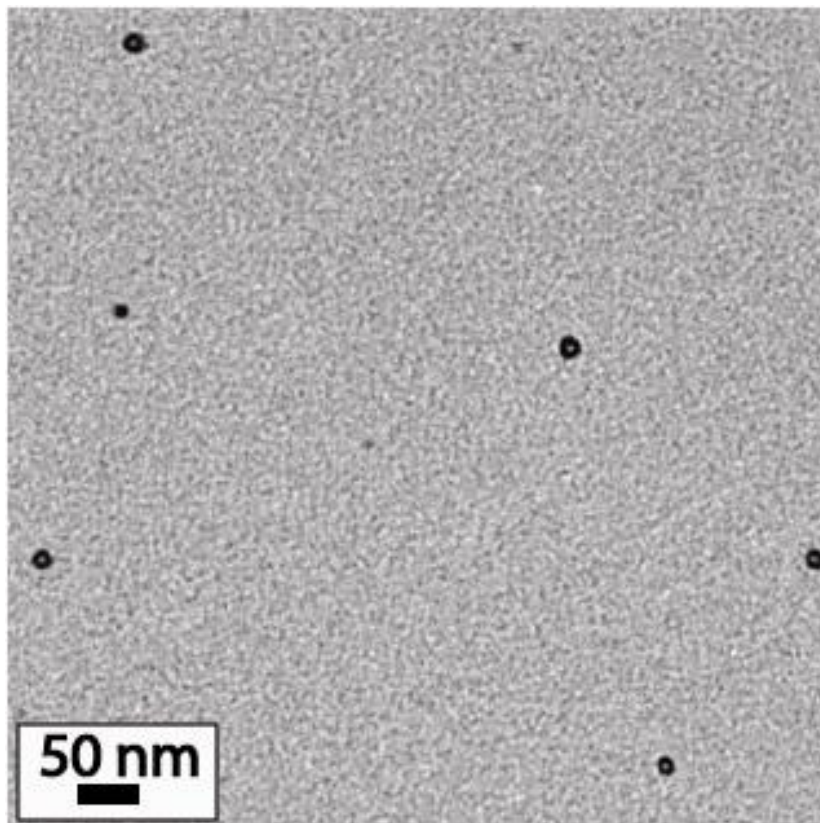


Figure S5: TEM image of Ni-Gr showing the formation of spherical particles rather than nanocages. Particle size is around 20-25 nm. This gives a clear idea of the important role played by nitrogen during the Ni-NGr nanocage synthesis.

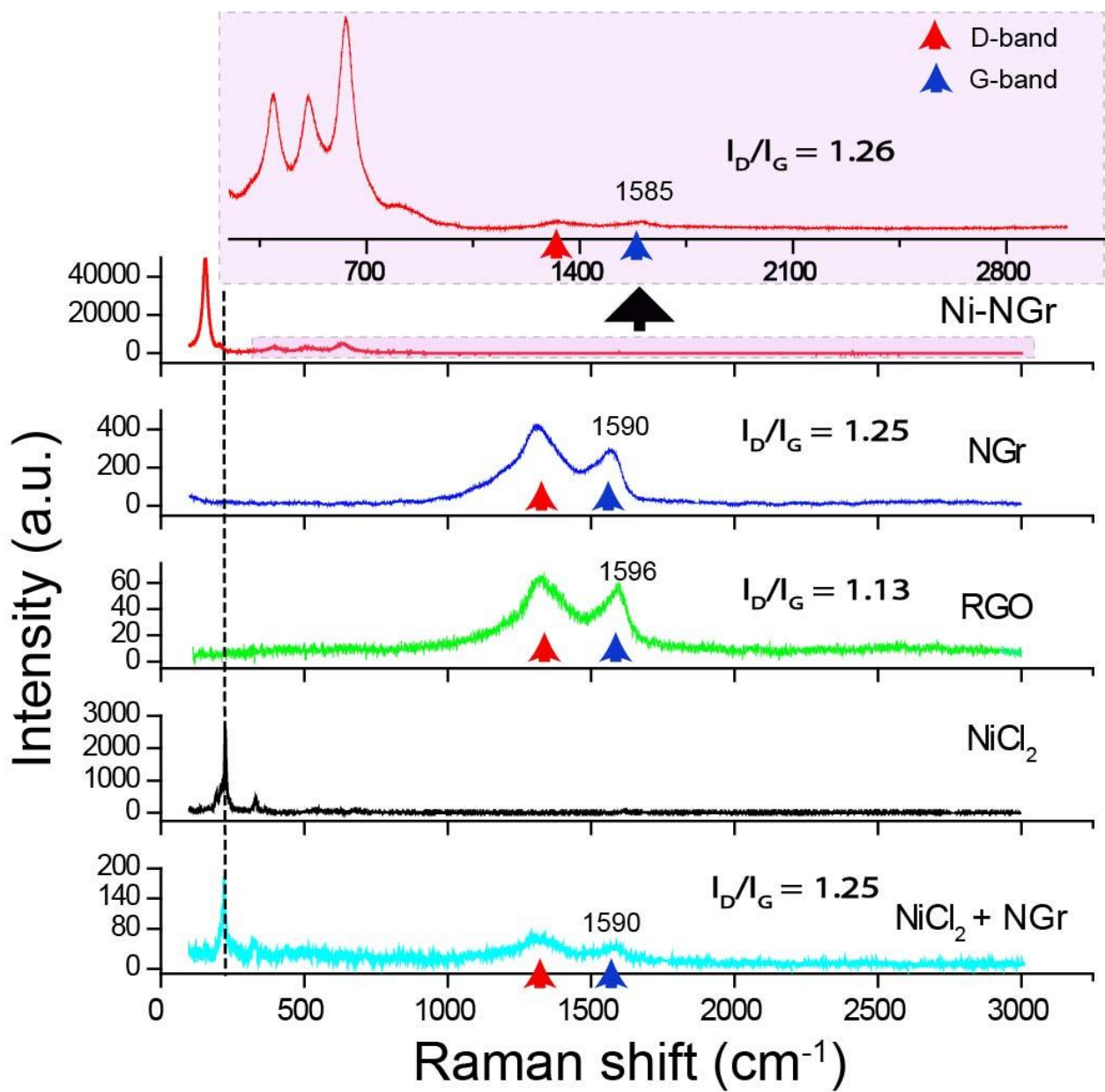


Figure S6: Comparative Raman spectra of RGO (Gr), NGr, NiCl₂, Ni-NGr, and physically mixed NiCl₂ and NGr (NiCl₂+NGr).

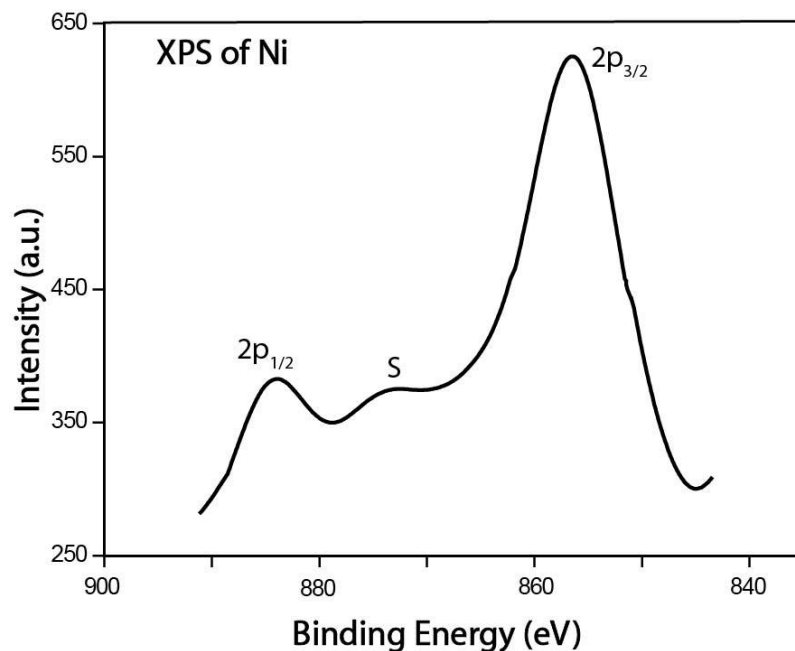


Figure S7: XPS of Ni of the NiCl_2 precursor used for the synthesis of Ni-NGr.

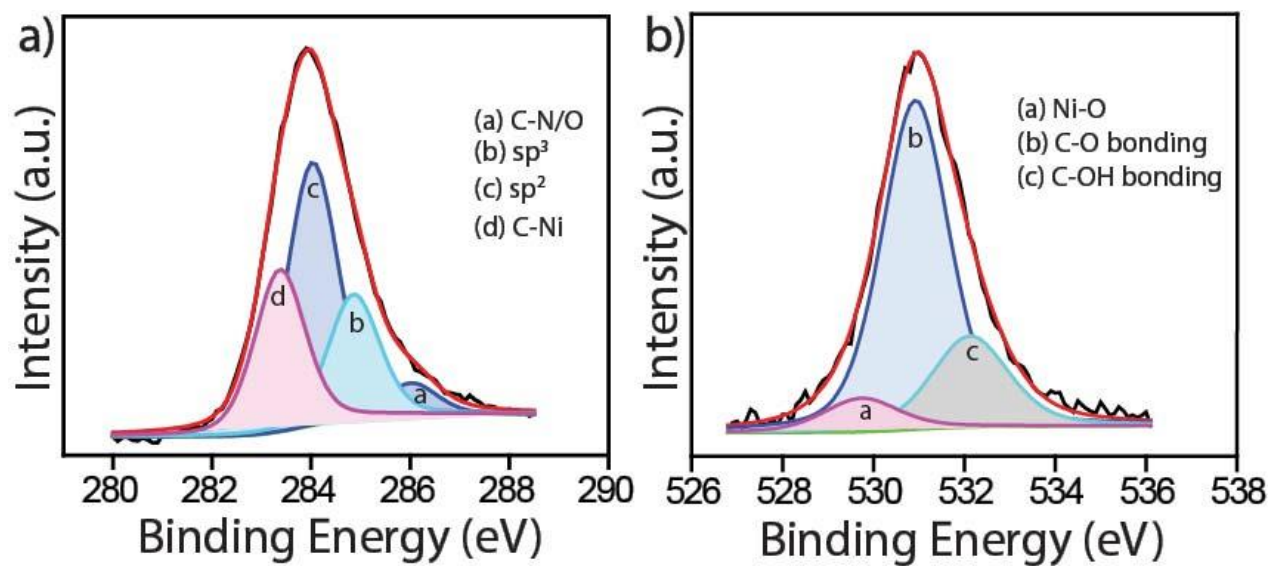


Figure S8: Deconvoluted XPS of a) C1s and b) O1s, of the Ni-NGr sample.

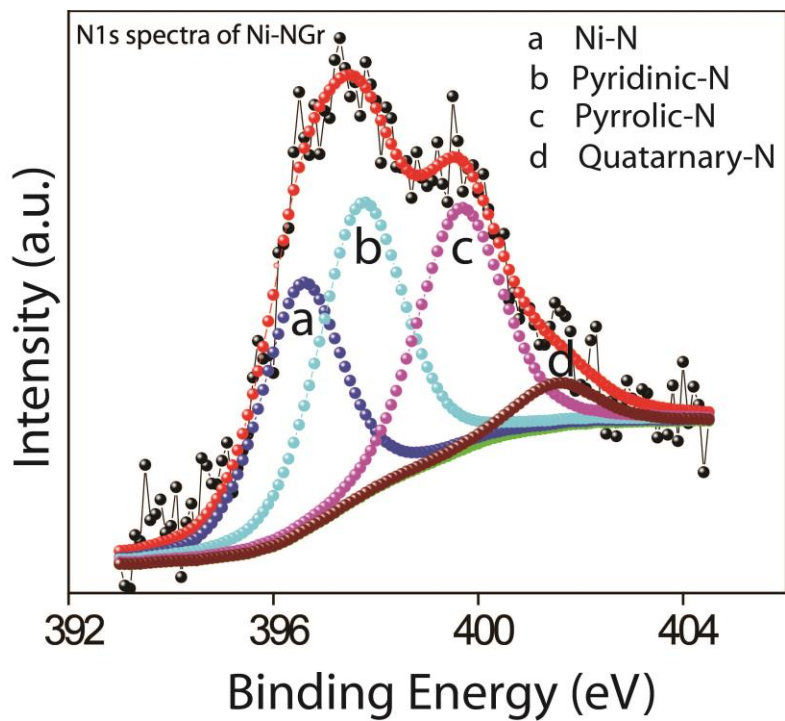


Figure S9: Deconvoluted N1s XPS of the Ni-NGr sample.

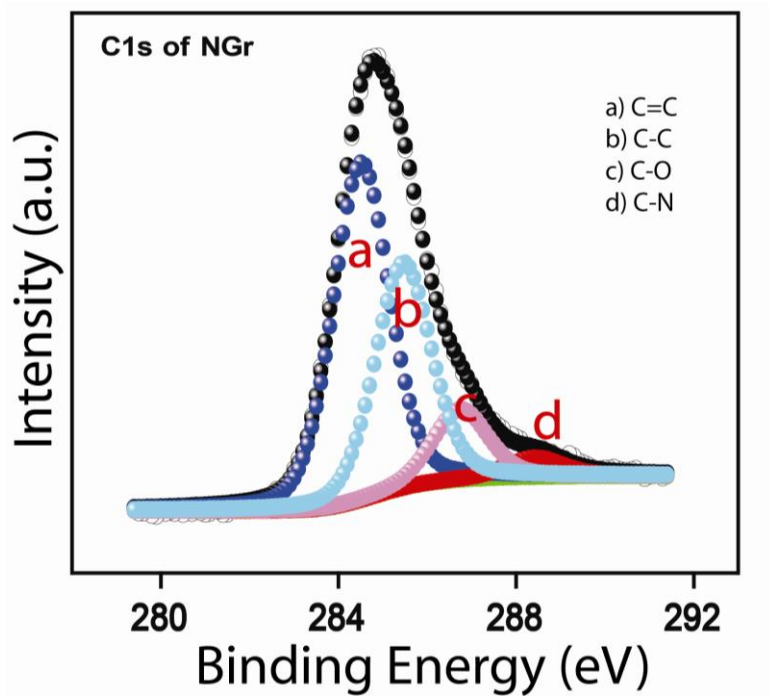


Figure S10: Deconvoluted C1s XPS of the NGr sample.

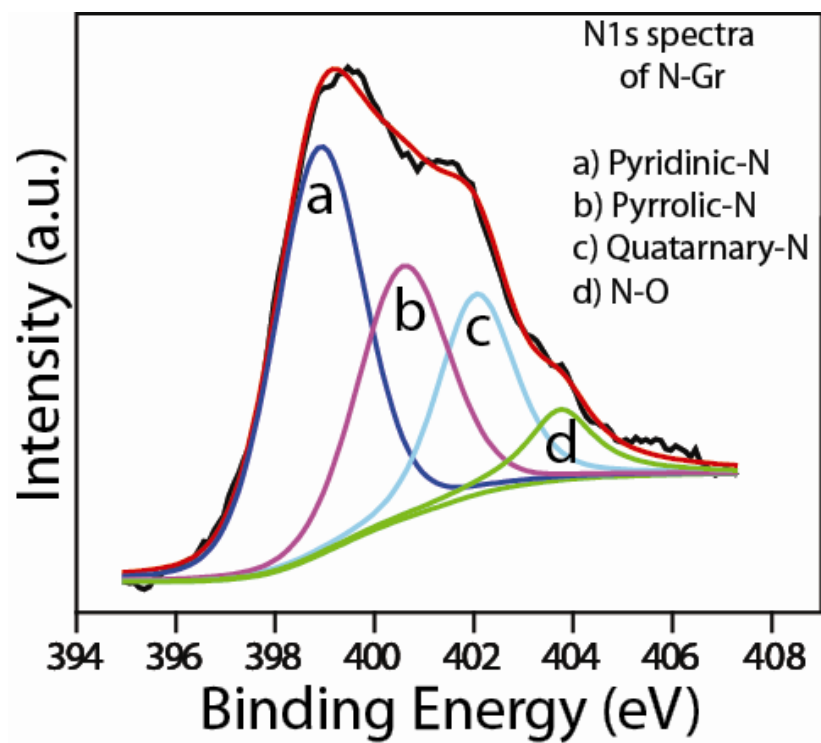


Figure S11: Deconvoluted N1s XPS of the NGr sample.

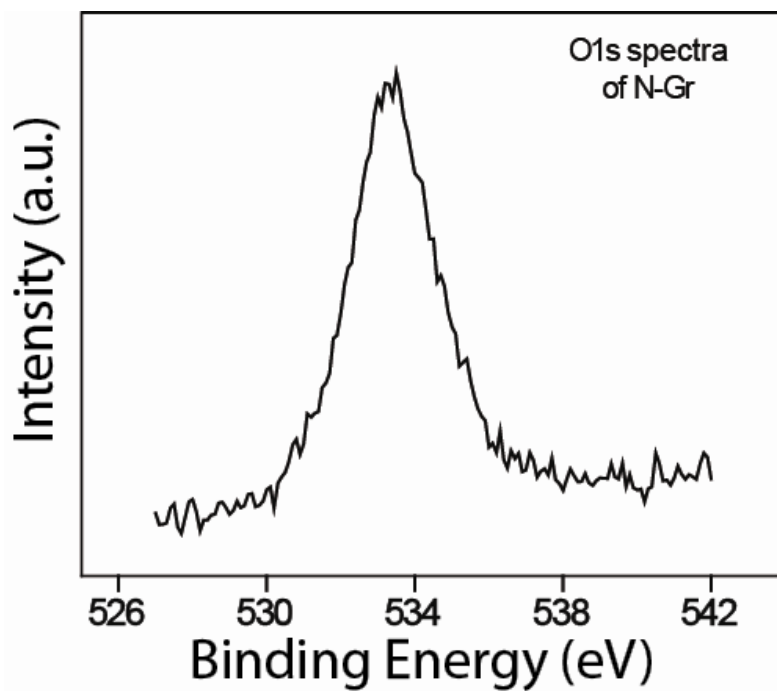


Figure S12: Deconvoluted O1s XPS of the NGr sample.

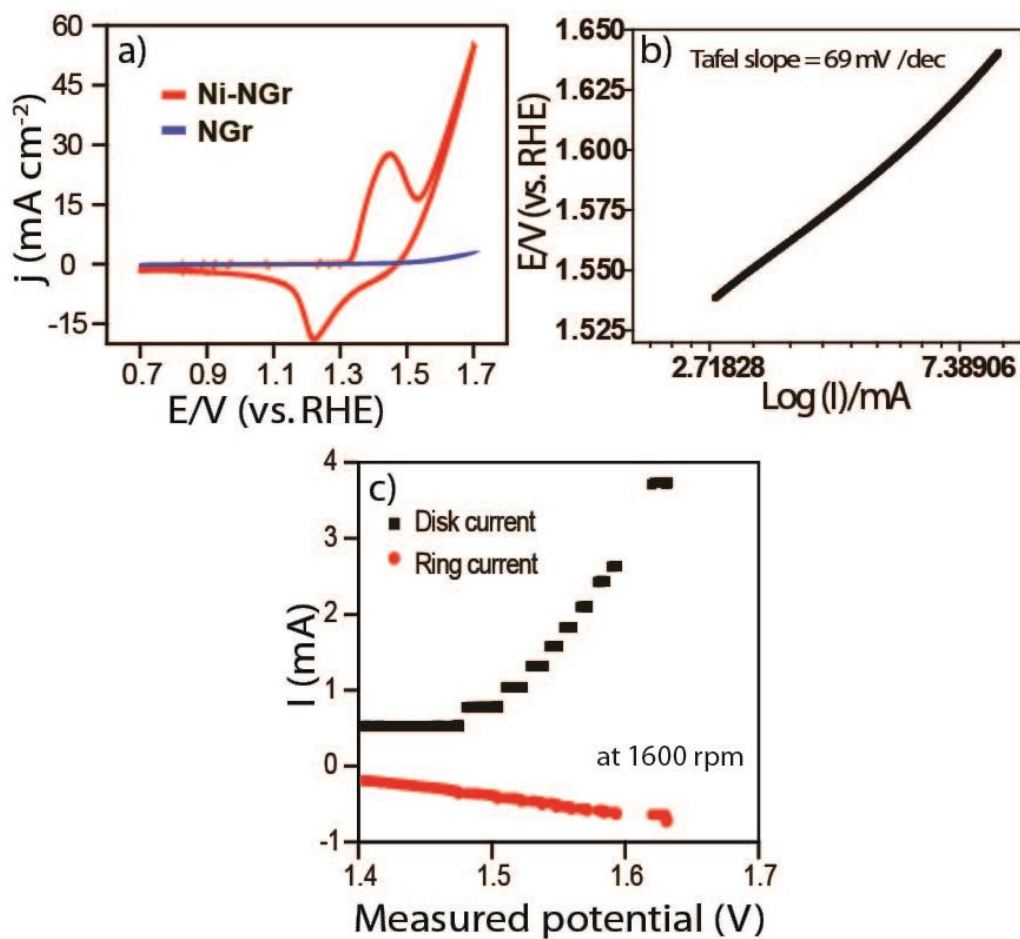


Figure S13: a) Comparative CV of NGr and Ni-NGr, performed at a scan rate of 50 mV/s, b) Tafel plot for oxygen evolution activity of Ni-NGr, and c) rotating-ring disk electrode (RRDE) study for OER of Ni-NGr nanocages, recorded in nitrogen saturated 0.1M KOH at 1600 rpm. The disk electrode is subjected to a series of current steps, and the corresponding potentials are measured.

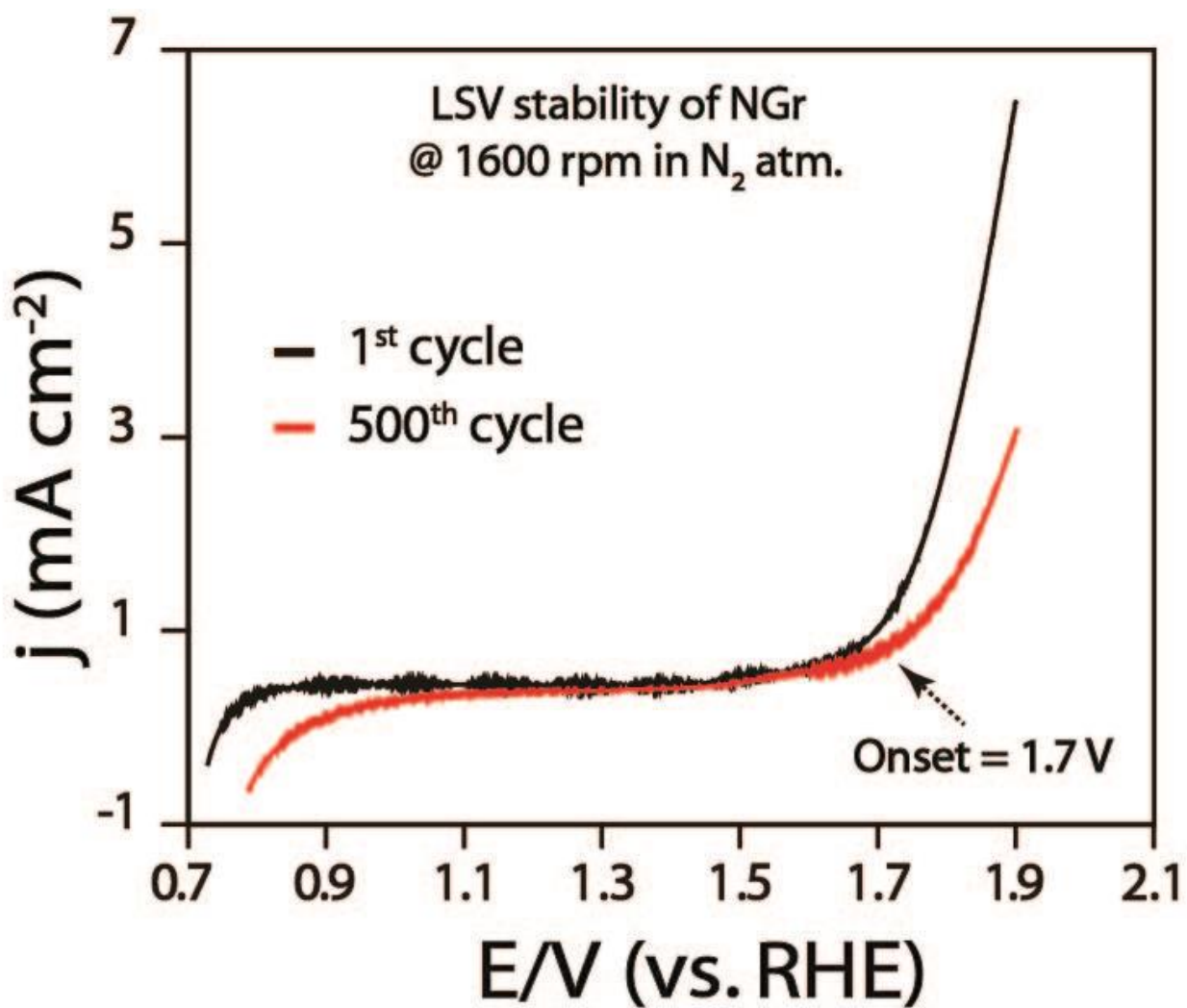


Figure S14: LSV OER stability of NGr recorded in nitrogen saturated 0.1M KOH at 1600 rpm. The overpotential is around 470 mV (at onset). The current is also very low for OER.

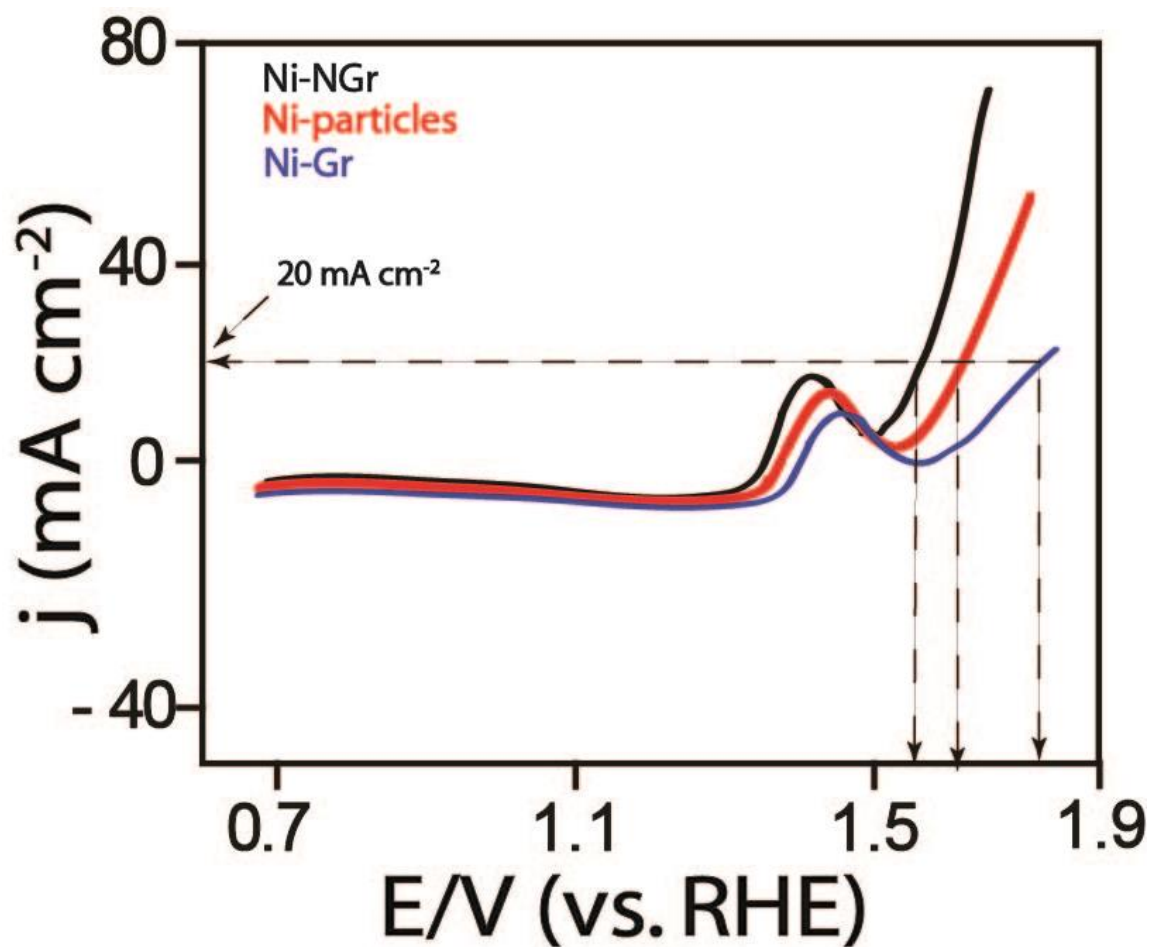


Figure S15: Comparative LSV of Nickel particles, Ni-Gr, and Ni-NGr recorded in nitrogen saturated 0.1M KOH at 1600 rpm. The calculated overpotential at 20 mAcm⁻² for Ni-particles, Ni-Gr and Ni-NGr is ~370, 570, and 290 mV. The OER current is seem to be in order of Ni-NGr > Ni-particles > Ni-Gr.

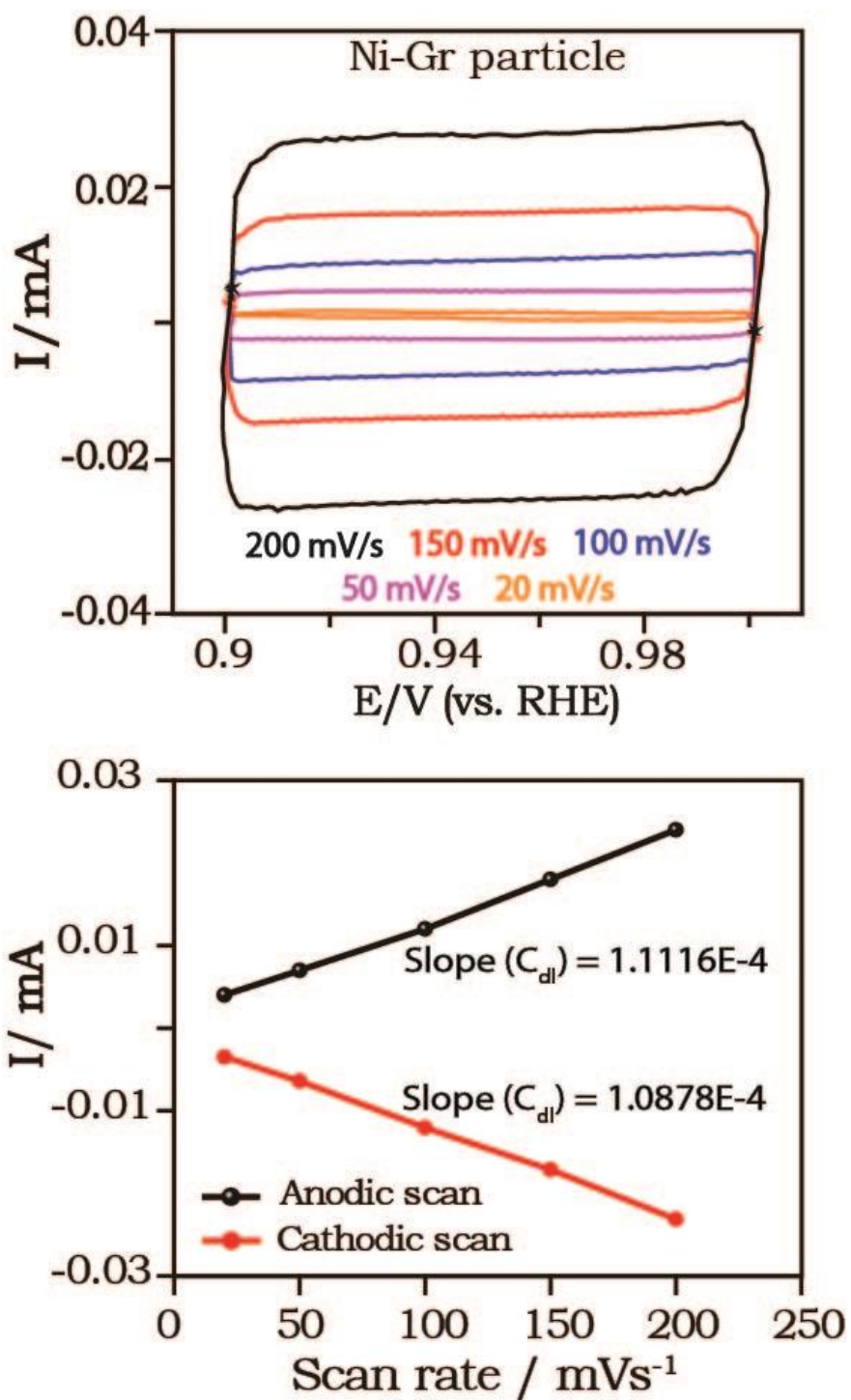
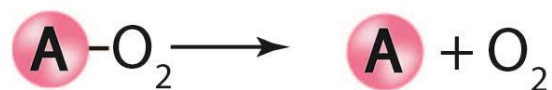
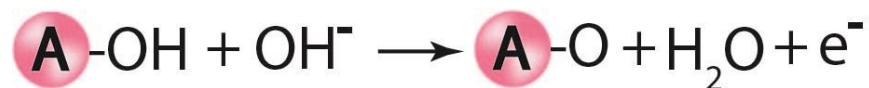


Figure S16: (Top) The capacitive CV of the Ni-Gr particles recorded with different scan rates, where no apparent faradaic process takes place. CV is performed in nitrogen saturated 0.1 M KOH; electrode geometrical area: 0.19625 cm^2 ; (bottom) plot of anodic and cathodic current vs. scan rate at 0.95 V (vs. RHE), and the calculated ESCA is 4.11 cm^2 .

3. Mechanism of OER in alkaline medium:



A is active center

Table S1: Desorption energy per carbon atom (E_{des}) and activation energy (ΔE_a) for carbon diffusion of nickel surface.³

| Surface plane | Surface energy (J/m ²) | Desorption energy (E_{des}) in eV | Activation energy (ΔE_a) in eV |
|---------------|---------------------------------------|---|---|
| 111 | 2.02 | 6.28 | ~0.4 |
| 100 | 2.23 | 7.61 | ~2.1 |
| 110 | 2.29 | 6.76 | ~0.4 |
| 311 | 2.31 | | |

Table S2: Reported specific capacitance (C_s) for Ni-based materials and platinum in alkaline medium.

| Ni-based electrocatalyst | Alkaline electrolyte conc. | C_s , mF cm ⁻² | Reference |
|--------------------------|----------------------------|-----------------------------|-----------|
| Ni | 1 M NaOH | 0.03 | 4 |
| Ni | 0.5 M KOH | 0.04 | 5 |
| Ni | 31% KOH | 0.03 | 6 |
| Ni | 4 N KOH | 0.022 | 7 |
| Ni-Co | 1 M NaOH | 0.026 | 8 |
| Pt | 1M KOH | 0.028 | 9 |
| Pt/C | 1M KOH | 0.03 | 10 |

Table S3: Reported overpotential values for Ni-based electrocatalysts.¹¹

| Electrocatalyst | Alkaline electrolyte conc. and catalyst synthesis method | Overpotential (mV) | Reference |
|----------------------------------|--|--------------------|--------------|
| NiO _x | 1 M NaOH (Electrochemical deposition on Ni substrate and reported at 16 mA/cm ²) | 420 | 12 |
| NiCeO _x | 1 M NaOH (Electrochemical deposition on Ni substrate and reported at 16 mA/cm ²) | 280 mV | 12 |
| NiCoO _x | 5 M KOH (Electrochemical deposited on Cu substrate and reported at 10 mA/cm ²) | 400 mV | 13 |
| NiCuO _x | 1 M NaOH (Electrochemical deposited onto Ni substrate and reported at 100 mA/cm ² and 80 ⁰ C) | 420 mV | 14 |
| NiFeO _x | 1 M NaOH (Electrochemical deposited onto Pt and reported at 100 mA/cm ²) | 290 mV | 15 |
| NiFe ₂ O ₄ | 1M KOH (Hard template method and reported at 10 mA/cm ²) | 360 mV | 16 |
| Ni-NGr nanocage | water-in-oil emulsion technique | 270 mV | Present work |

4. References

1. Marcano, D. C.; Kosynkin, D. V.; Berlin, A.; Sinitskii, Z.; Sun, A.; Slesarev, L. B.; Alemany, W.; Tour, J. M. *ACS Nano*, **2010**, *8*, 4806-4814.
2. Bard, A. J.; Faulkner, L. R. *Electrochemical Methods: Fundamentals and Applications, Second Edition*, Wiley, ISBN: 978-81-265-0807-5.
3. Hong, S.; Shin, Y-H.; Ihm, J. *Jpn. J. Appl. Phys.*, **2002**, *41*, 6142-6144.
4. Lasia, A.; Rami, A.; *J. Electroanal. Chem.* **1990**, *294*, 123-141.
5. Gu, P.; Bai, L.; Gao, L.; Brousseau, R.; Conway, B. E. *Electrochim. Acta*, **1992**, *37*, 2145.
6. Gagnon, E. G. *J. Electrochem. Soc.* **1973**, *120*, 1052-1056.
7. Weininger, J. L.; Breiter, M. W. *J. Electrochem. Soc.* **1963**, *110*, 484-490; *J. Electrochem. Soc.* **1964**, *111*, 707-712.
8. Wu, G.; Li, N.; Zhou, D.-R.; Mitsuo, K.; Xu, B.-Q. *J. Solid State Chem.* **2004**, *177*, 3682-3692.
9. Bai, L.; Gao, L.; Conway, B. E. *J. Chem. Soc., Faraday Trans.* **1993**, *89*, 235-242.
10. Fournier, J.; Brossard, L.; Tilquin, J.-Y.; Cote, R.; Dodelet, J.-P.; Guay, D.; Menard, H. J. *Electrochem. Soc.* **1996**, *143*, 919-926.
11. McCrory, C. C. L.; Jung, S.; Peters, J. C.; Jaramillo, T. F. *J. Am. Chem. Soc.* **2013**, *135*, 16977.
12. Corrigan, D. A.; Bendert, R. N. *J. Electrochem. Soc.* **1989**, *136*, 723-728.
13. Ho, J. C. K.; Piron, D. L. *J. Appl. Electrochem.* **1996**, *26*, 515-521.
14. Li, X.; Walsh, F. C.; Pletcher, D. *Phys. Chem. Chem. Phys.*, **2011**, *13*, 1162-1167.
15. Merrill, M. D.; Dougherty, R. C. *J. Phys. Chem. C* **2008**, *112*, 3655-3666.
16. Landon, J.; Demeter, E.; Inoglu, N.; KEturakis, C.; Wachs, I. E.; Vasic, R.; Frenkel, A. I.; Kitchin, J. R. *ACS Catal.* **2012**, *2*, 1793-1801.
17. Hurst, J. K. *Science*, **2010**, *328*, 315; Kanan, M. W.; Nocera, D. G. *Science*, **2008**, *321*, 1072.